

# Application of a Cross-linked Polyacrylic Acid- Polyethylene Oxide (PAA-PEO) Copolymer as a Binder for Si@C@PDA Composite Anode Materials in Li-ion Batteries

Shibin Liu\*, Xiangcai Meng, Jing Wang, Jianwei Xu, Hongbo Li

School of Materials Science and Engineering, Jiamusi University, Jiamusi 154007, China

\*E-mail: [christainvieri@126.com](mailto:christainvieri@126.com)

Received: 9 September 2021 / Accepted: 17 November 2021 / Published: 5 January 2022

In this paper, a PAA-PEO cross-linking binder was prepared by the copolymerization method and used in Si@C@PDA composite anode materials for Li-ion batteries. The phenolic hydroxyl in PAA-PEO and the hydroxyl in the self-polymerized PDA on the surface of Si@C can form a three-dimensional cross-linking binding system with strong hydrogen bonds. Compared with the traditional binder, PAA-PEO has higher adhesion and conductivity. The structure of Si@C@PDA-PAA-PEO was successfully determined by IR and XPS. The electrochemical results show that PAA-PEO can significantly improve the cycle stability of the Si@C@PDA composite negative electrode material, and can maintain a 600 mAgh<sup>-1</sup> stable cycle 200 times under a 1000 mAgh<sup>-1</sup> current density, and the first coulombic efficiency is 89.4%.

**Keywords:** Li-ion battery, Crosslinking binder, dopamine, electrochemical properties.

## 1. INTRODUCTION

As an important part of lithium-ion batteries, binders play an important role in the electrochemical performance of electrodes [1-3]. Polyvinylidene fluoride (PVDF), a traditional binder, is widely used in commercial batteries because of its good thermal stability and easy dispersion. However, it is not suitable for silicon-based anode materials, mainly because PVDF and silicon particles do not form hydrogen bonds but only interact via simple van der Waals forces. This type of combination cannot effectively alleviate the volume stress imposed by lithium ions on the negative Si material during the charging and discharging process, and obvious fractures and falling off occur, thus affecting the cycle stability of lithium-ion batteries [4,5]. In addition, the process of PVDF synthesis is complex, and the raw materials often include toxic N-methyl-pyrrolidone (NMP), which causes severe environmental

pollution [4]. Therefore, it is a hot spots to study the binders that are suitable for silicon-based anode materials, environmentally friendly, low cost, and suitable for mass production.

To address the above shortcomings of the traditional binder PVDF, in recent years, researchers have found that sodium alginate (Alg), polyacrylic acid (PAA), polyvinyl alcohol (PVA), sodium carboxymethylcellulose (CMC), styrene butadiene rubber (SBR), and other water-based binders with hydrogen bonds can effectively improve the electrochemical performance of silicon anode materials [6-8]. Researchers found that a water-based binder containing a large number of carboxyl (-COOH) or COONa groups can form hydrogen bonds with -OH, the hydroxyl group in its molecule can react with the hydroxyl group in the active substance to form hydrogen bonds, and the van der Waals force between hydrogen bonds can improve the stability of the electrode, so as to improve the binding force between the active material and the conductive agent, and improve its cycle stability [9]. Although these binders can solve the problem of the attenuation of Si negative electrode materials, linear structural binders with a single structure will have irreversible slip with Si particles [10,11], which will cause the active materials to crack or peel off on the collecting fluid. Therefore, researchers have proposed the synthesis of a composite cross-linking binder as the binder of Si negative electrode materials. The binder with this structure can form a deformable three-dimensional network structure in the process of cross-linking, which can form a multipoint interaction with the silicon surface, effectively prevent the separation of silicon particles, and further improve the cycle stability of the battery. Song et al. [12] prepared a PAA-PVA cross-linking binder by in situ thermal cross-linking. The cross-linking binder contains a large number of carboxyl and hydroxyl functional groups, which can react with the hydroxyl groups on the surface of silicon to form a strong covalent bond, stabilize the structure of the electrode, and improve the cycling stability of the negative material of Si. Lim et al. [13] prepared a cross-linking binder with a network structure by physical cross-linking of PAA and PEG. The results show that the first coulombic efficiency of the Si anode material is 99.1%, and the capacity of 740 mAh<sup>-1</sup> is maintained after 100 cycles.

In recent years, mussels of marine bivalve mollusks have been shown to secrete a kind of super-strong mucus, that can be closely adhere to the surface of reefs and hull [14]. The main component of mucus is mussel adhesion protein (MAPs), which solidifies rapidly in humid environments and interacts strongly with the surface of matrix material. MAPs contain a large amount of protein mfp-5 (Mytilus foot protein 5), which contains approximately 30% of L-dopa and 15% lysine residues, and is the key factor for adhesion effects [15-17]. Inspired by the adhesion of mussels, researchers found that dopamine, as a catechol derivative of L-dopa, can self-polymerize to form polydopamine (PDA) under alkaline conditions. There are many amino and bisphenol structures on the surface of PDA, which can well simulate the adsorption effect of mussels.

Poly (ethylene oxide) (PEO) is often used in solid electrolytes in lithium-ion batteries because of its high conductivity [18]. At the same time, the ether group on PEO is also considered to be able to cross-link with hydroxyl groups. PEO-based polymers are often used as the binder of anode materials for lithium-ion batteries. Due to its excellent electronic transmission performance, the conductivity of silicon anode material can be significantly improved [19].

In conclusion, a simple and effective PAA-PEO cross-linking binder with a three-dimensional network structure was developed. A layer of self-polymerized polydopamine was coated on the surface

of the Si@C composite anode material. A solid three-dimensional network structure was formed by combining the amino and bisphenol structure in PDA with the hydrogen bond of carboxyhydroxy in the PAA-PEO cross-linking binder. The electrochemical test results showed that the Si@C@PDA-PAA-PEO electrode material has excellent electrochemical performance and cycle stability. For the first time, the coulomb efficiency is 89.4%. It can maintain a stable cycle of 600 mAgh<sup>-1</sup> for 200 times under a 1000 mAgh<sup>-1</sup> current density.

## 2. EXPERIMENTAL MATERIALS AND METHODS

### 2.1 Preparation of the Si@C@PDA-PAA-PEO electrode material

#### 1) Synthesis of the PAA-PEO cross-linking binder

PAA and PEO were added at a molar ratio of 4:1, and then THF was added to mix them evenly. Then, DMAP and DCC were added. After stirring at 50 °C for 168h, dicyclohexylurea (DUC) was removed by filtration, and then the precipitate was washed with ethyl acetate. To obtain the PAA-PEO copolymer, excess PEO was removed and dried in a vacuum drying oven at 80 °C for 2h. The specific synthesis process is shown in Fig. 1.

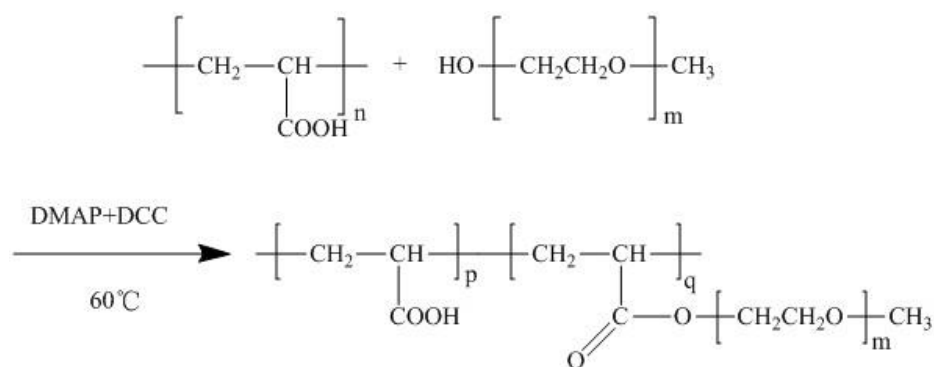


**Figure 1.** Synthesis of the PAA-PEO comblike copolymer

#### 2) preparation of Si@C@PDA-PAA-PEO electrode

#### 2) Preparation of the Si@C@PDA-PAA-PEO electrode

Si(0.5g, Ningbo Jinlei Nano Materials Technology Co., Ltd.), 0.5g POLY-4-(2-methylamino) Benzene-1, 2-bisphenol (dopamine) 1:1 were coated, added to 250 ml aqueous solution, ultrasonic cleaning for 30 minutes, magnetic stirring for 8 hours, adding 0.173g tris, stirring with deionized water evenly. The Si@poly 4-(2-methylamino) benzene-1,2-bisphenol (Si@PDA) precursor was prepared by vacuum filtration, three times and drying in a vacuum oven at 80 °C for 24 hours. The prepared Si@PDA precursor was placed in a tubular furnace and kept at 800 °C for 2 hours at a rate of 5 °C/min. The coated silicon carbon composite (Si@C) was prepared. Then 0.3g dopamine was added, and the process of precursor coating was repeated to obtain Si@C@PDA. The Si@C@PDA-PAA-PEO battery system was

prepared by grinding the prepared Si@C@PDA active material, conductive agent, and PAA-PEO cross-linking adhesive on the copper foil. The specific synthesis process is shown in Fig. 2.

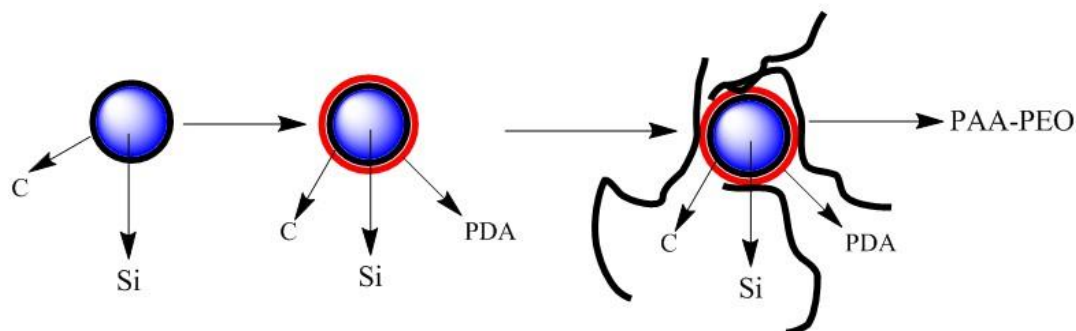


**Figure 2.** Synthesis diagram of Si@C@PDA-PAA-PEO

## 2.2 Materials characterization

Fourier transform infrared spectroscopy (FTIR) spectra of the samples were obtained by using Nicolet IS 10(IS50FT-LR., USA) in a range of 400–4500  $\text{cm}^{-1}$ . The morphology of the Si@C composite materials was characterized using a scanning electron microscopy (SEM, S4800, Hitachi, Japan). Raman spectra were recorded on a spectrograph microRaman system (LabRam HR Evolution, France)

## 3. RESULTS AND DISCUSSION

### 3.1 Structure and properties of the materials

To verify the successful polymerization of PAA-PEO and the successful preparation of the Si@C@PDA-PAA-PEO electrode, we tested Si@C, PDA-PAA-PEO and the coated Si@C@PDA-PAA-PEO by IR, as shown in Fig. 3. Fig. 3a) is the infrared spectrum comparison diagram of Si@C and Si@C@PDA, which can be compared with the infrared spectrum of Si@C. After being wrapped by a small amount of PDA, there is a strong absorption peak due to the N-H vibration at  $1645 \text{ cm}^{-1}$ , corresponding to other peaks related to C=C, C-N, and C-O vibrations at  $1508$ ,  $1307$ , and  $1221 \text{ cm}^{-1}$ , respectively. These characteristic peaks proved that polydopamine was successfully self-polymerized on the surface of Si@C again, and the Si@C@PDA material was obtained by a second coating. Fig. 3b) shows the infrared spectra of the PAA and PAA-PEO cross-linking binders. It can be seen from the figure that there are absorption peaks near  $3446 \text{ cm}^{-1}$  and  $2870 \text{ cm}^{-1}$ , which are mainly due to the tensile properties of O-H and C-H. The absorption peak at  $1720 \text{ cm}^{-1}$  is due to the tensile properties of C=O, and the vibration absorption peak of  $-\text{CH}_2$  appears at  $1464 \text{ cm}^{-1}$ . The two absorption peaks at  $1455 \text{ cm}^{-1}$  and  $1351 \text{ cm}^{-1}$  are mainly due to the shear vibration of O and  $-\text{CH}_2$ . PAA has an absorption peak caused by tensile hydrogen bonds near  $3600\text{-}2500 \text{ cm}^{-1}$ . Compared with the infrared spectrum of PAA, the absorption intensity of PAA-PEO increases at  $2870$  and  $1250 \text{ cm}^{-1}$ , and new absorption peaks appear at  $1455 \text{ cm}^{-1}$ ,  $1351 \text{ cm}^{-1}$ ,  $951 \text{ cm}^{-1}$  and  $844 \text{ cm}^{-1}$ . The results showed that in the presence of a catalyst, PEO and PAA were esterified and successfully grafted onto the PAA chain. Fig. 3 c) shows the infrared spectra of the PAA-PEO and Si@C@PDA-PAA-PEO cross-linking binders. The cross-linking reaction between

Si@C@PDA and PAA-PEO was confirmed by comparative spectra. It can be seen from the figure that the peak value of the N-H deformation vibration ( $1645\text{ cm}^{-1}$ ) disappears in the Si@C@PDA-PAA-PEO electrode, indicating that N-H in Si@C@PDA reacts with COOH in PAA-PEO.

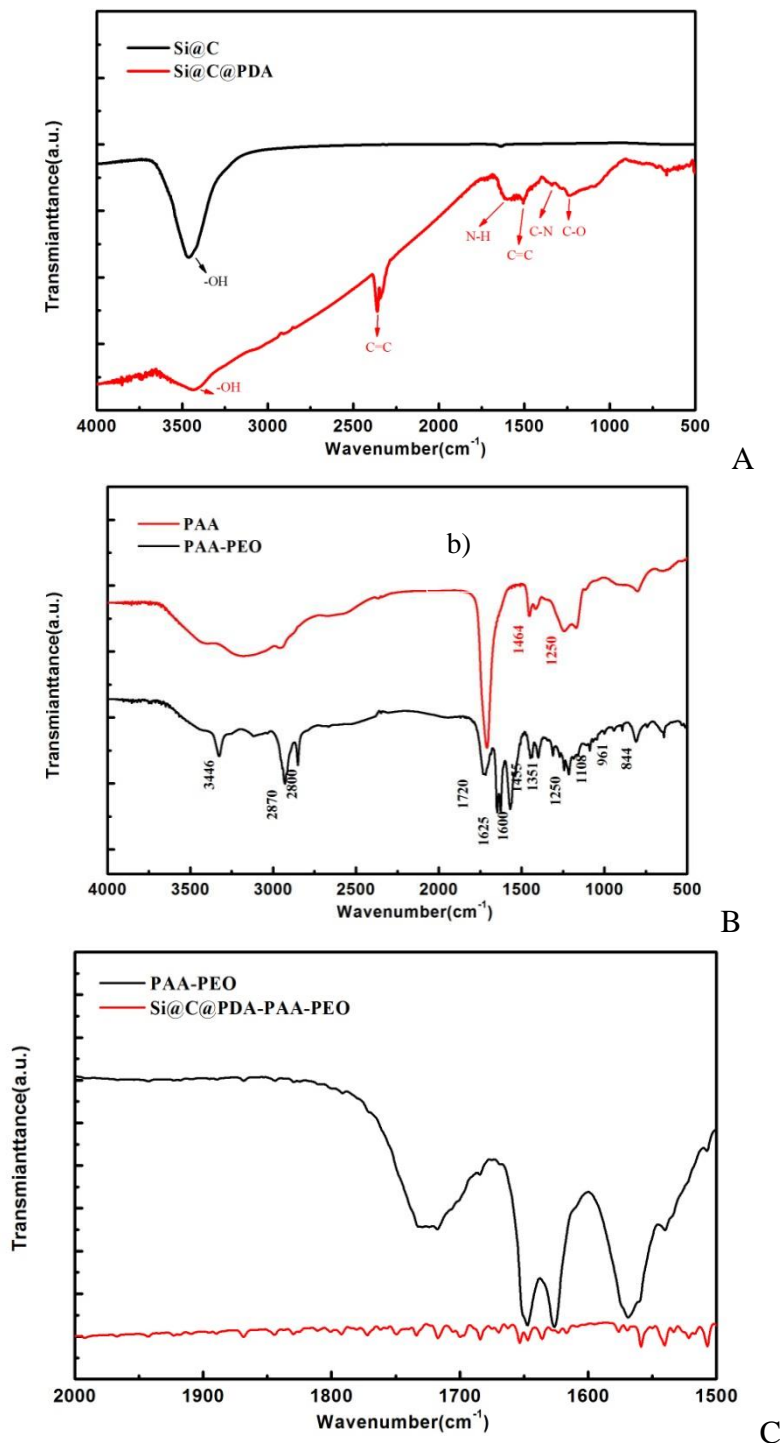


**Figure 3.** FTIR spectra of Si@C@PDA , PAA-PEO and Si@C@PDA-PAA-PEO

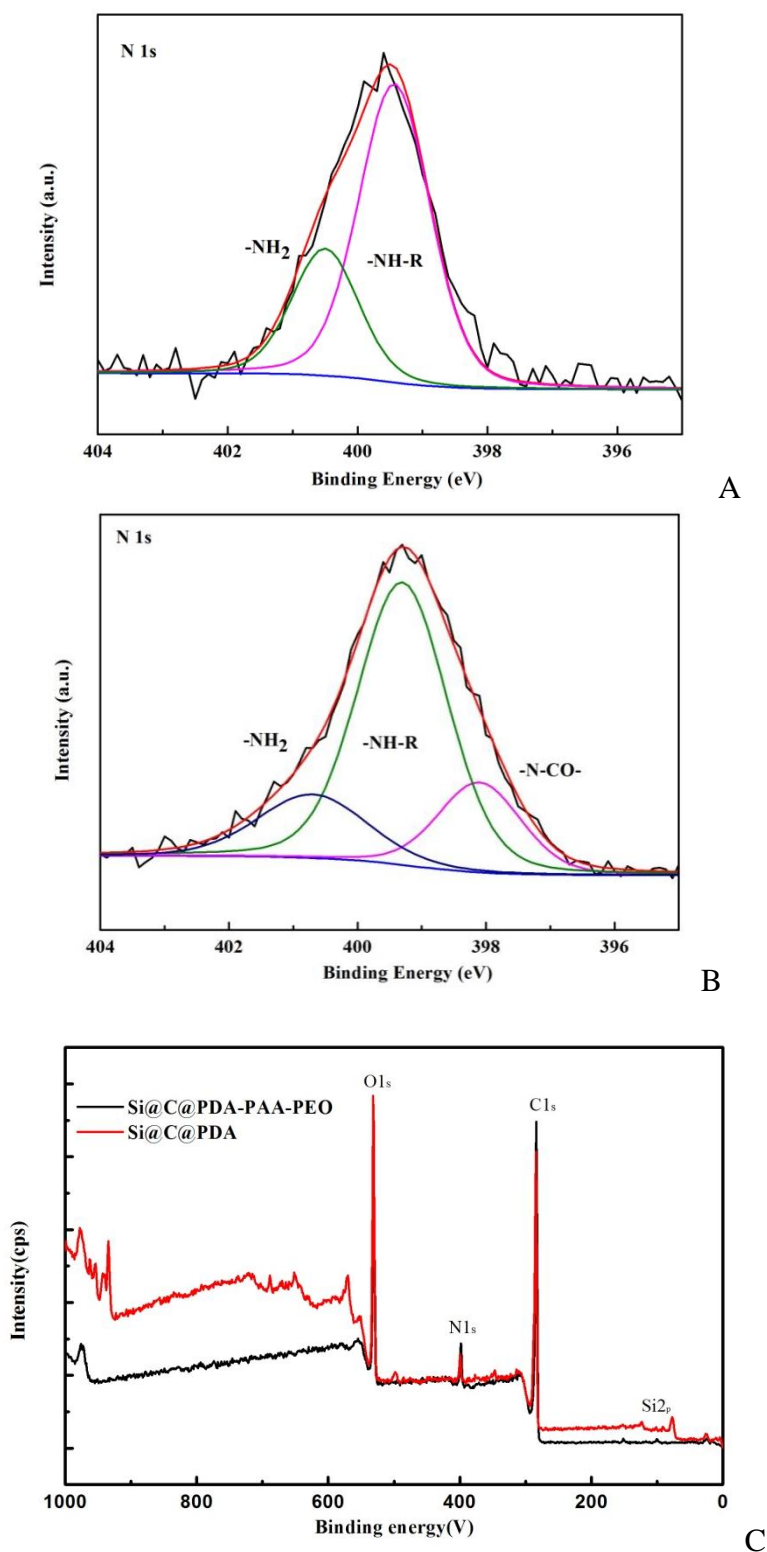


**Figure 4.** High-resolution XPS map of the n1 s region of Si@C@PDA and Si@C@PDA-PAA-PEO

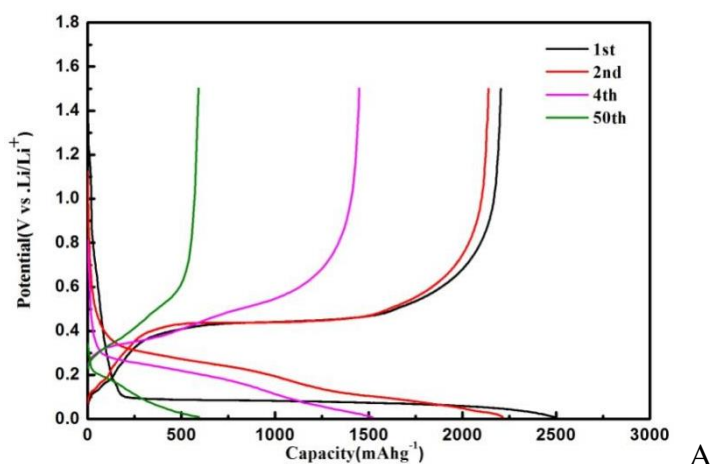
The deviation of the C=O peak in PAA-PEO(1714 cm<sup>-1</sup>) and Si@C@PDA electrode (1700 cm<sup>-1</sup>) also indicates that some carboxyl groups in PAA-PEO have been converted into amides. All these characteristic peaks indicate that Si@C@PDA-PAA-PEO was synthesized.

To further study the reaction between Si@C@PDA and PAA-PEO, we tested Si@C@PDA particles and Si@C@PDA-PAA-PEO electrodes by XPS.

As shown in Fig.4a) that the N1s region of Si@C@PDA matches the two peaks of primary (-NH<sub>2</sub>) and secondary (-NH-R) amine functional groups. In Fig. 4b), the N1s spectrum of the Si@C@PDA-PAA-PEO electrode shows a peak corresponding to tertiary amine (-NR-CO-) at 399.6 eV. Fig. 4c) XPS map. According to the chemical structure of dopamine, the -NH<sub>2</sub> and -NH-R peaks are related to PDA, and the -NR-CO- peaks are due to the condensation reaction between -NH-R in PDA and -COOH in PAA. Therefore, we conclude that a covalent amide bond is formed between PAA and PDA.

### 3.2 Electrochemical performance tests

To test the influence of the cross-linking binder on the cycling stability of the Si@C@PDA negative electrode material, we selected PVDF and Alg as the control groups to carry out charge-discharge tests. Fig. 5 shows the charge-discharge curve of lithium-ion batteries assembled with different binders. The charge-discharge curves of the 1st, 2nd, 4th, and 50th cycles are shown in the figure. The first four current densities were 100 mA g<sup>-1</sup>, 1000 mA g<sup>-1</sup> after 4 cycles. It can be seen from the figure that when the first discharge voltage drops to 0.2 V, the lithium silicon alloy will undergo the lithium process, resulting in a longer discharge platform for all three groups of samples when the voltage platform is lower than 0.2 V. When the number of electrode increases, the polarization degree of the electrode also increases, the discharge voltage plateau decreases, and the charging voltage plateau increases. It can be seen from the figure that after 50 cycles of the electrode material prepared with PVDF as the binder, the discharge platform is reduced to 1 V, and the polarization effect is the most serious, while the polarization effect of the electrode material prepared with Alg and PAA-PEO as the binders is smaller, which shows that compared with PVDF, the water-based binder with hydrogen bond, Alg and PAA-PEO, is more suitable as the binder of Si@C@PDA composite negative electrode material.



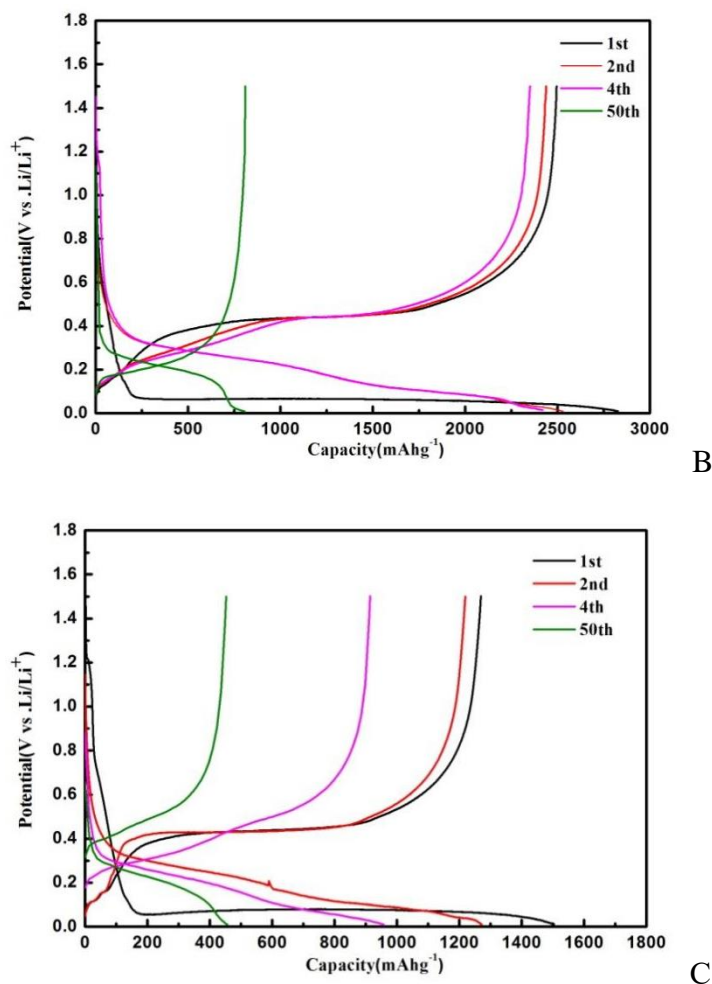


**Figure 5.** Charge-discharge curves of Si@C composite anode materials prepared by different binders (a: PVA; b: SCMC; c: Alg)

Fig. 6 shows the effect of three binders on the cycle performance of Li-ion batteries. It can be seen from the figure that the electrode materials prepared with the three kinds of binders all reflect a relatively high first reversible specific capacity. For Si@C-PVDF, the first reversible capacity was 2392 mAhg<sup>-1</sup>. After four cycles, the reversible specific capacity decreased to 1541 mAhg<sup>-1</sup>. The capacity of Si@C-PVDF decays rapidly when the current is added to 1000 mA g<sup>-1</sup> after 4 cycles, and the capacity decays nearly to 0 after 200 cycles. It can also be concluded that PVDF is not suitable for the binder of Si@C composite anode material. Compared with PVDF, the Si@C@PDA composite negative electrode material with an Alg water-based binder and PAA-PEO cross-linked binder has excellent cycle performance. Its first charge and discharge capacities are 2288 mAhg<sup>-1</sup> and 2253 mAhg<sup>-1</sup> respectively. After 100 cycles, the capacity is still stable and high. Compared with Alg and PAA-PEO, Si@C@PDA prepared with PAA-PEO as the binder has the highest first coulombic efficiency, up to 89.4%, and the second cycle coulombic efficiency increases rapidly to 95.6%. After 200 cycles, the coulombic efficiency remained above 99%. However, after 20 cycles, the capacity of the negative electrode material with Alg as the binder decreased sharply, and after 200 cycles, the capacity was only kept at 300 mAhg<sup>-1</sup>.

<sup>1</sup>. This shows that the volume expansion of the Si@C@PDA composite negative electrode material with Alg as the binder will cause irreversible damage to the negative electrode material with continuous charging and discharging, resulting in capacity degradation. For the electrode with PAA-PEO as the binder, when the current increases to  $1000 \text{ mA g}^{-1}$ , its capacity is at  $1307.4 \text{ mAh g}^{-1}$ , and continues to decrease as the number of cycles increases. It tends to be stable after about 20 cycles. After 200 cycles, its capacity remains at  $600 \text{ mAh g}^{-1}$ , with almost no attenuation. The cycle performance of the Si@C@PDA-PAA-PEO electrode is better than that of Si@C@PDA-PVDF and Si@C@PDA-Alg. This is mainly due to the hydrogen bond between PAA-PEO and PDA coated on the Si@C surface. PAA-PEO contains a large number of carboxyl groups, which can form strong hydrogen bonds with the hydroxyl groups of PDA coated on the surface of Si, greatly alleviating the irreversible damage caused by the volume expansion of Si in the process of charge and discharge [20]. Meanwhile, the hydroxyl groups of a large number of catechol functional groups contained in PEO can also interact with the hydroxyl groups in PDA, which can greatly improve the adhesion of PAA-PEO and ensure the expansion and recovery of silicon. During condensation, it will not lose contact with the conductive agent and collecting fluid and keep the integrity of the electrode [21] to further stabilize the structure of the Si negative electrode so that it can stably circulate 200 times without attenuation.

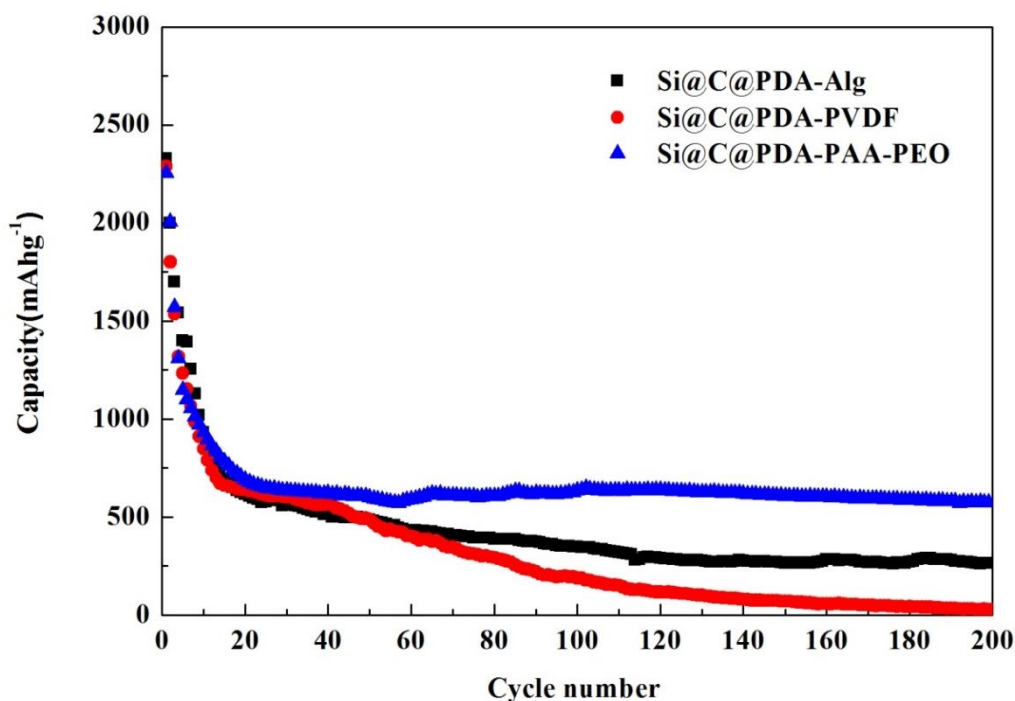


**Figure 6.** Cyclic Properties of Si@C@PDA Composite Anode Materials Prepared with Different Binders

To further study the influence of the binders on the electrochemical performance of Si@C@PDA composite negative electrode materials, the above binders, Alg and PAA-PEO, which are suitable for Si@C@PDA composite negative electrode materials, are selected for a rate performance test, as shown

in Fig. 7. With increasing magnification, the electrode capacities of the two materials maintain good cycle stability. At 0.1C and 0.25C, the discharge specific capacities of the two materials are the same, but when the current is above 0.5C, Si@C@PDA-Alg will have a large attenuation, while Si@C@PDA-PAA-PEO has a small attenuation. When the magnification is back to 0.5C, the electrode capacities can return to 1500 mA $h^{-1}$ . It can be concluded that both of them can be used as excellent binders for Si@C composite anode materials. Si@C-Alg is more suitable for cycles with small magnification, while Si@C@PDA-PAA-PEO can still circulate stably at large magnification.

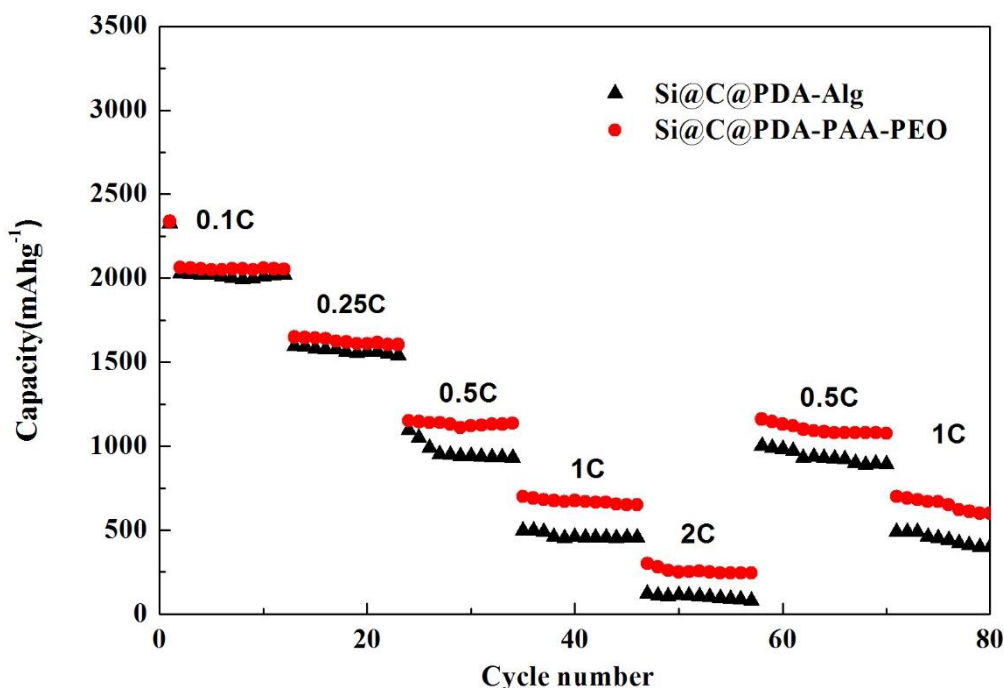


**Figure 7.** Cyclic performance of Si@C@PDA-Alg and Si@C@PDA-PAA-PEO electrodes at different rates

Fig. 8 shows the AC impedance map test of Si@C@PDA-PAA-PEO and Si@C-Alg under different cycles. It can be seen from the figure that the impedance spectrum of the composite negative electrode material prepared by two kinds of binders is composed of two semicircles (RF in the high-frequency region and RCT in the low-frequency region) and oblique lines [22]. The semicircle in the high-frequency region corresponds to the interface impedance, i.e., the formation process of SEI film. The semicircle in the low-frequency region corresponds to the charge transfer impedance. The oblique line is the lithium-ion diffusion impedance. It can be seen from the figure that with the increase of the number of cycles, the semicircles corresponding to the high-frequency and low-frequency regions of the composite anode materials prepared with two kinds of binders are reduced to varying degrees, which shows that with the continuous insertion/removal of lithium ions during the cycle, part of lithium-ion consumption remains in the anode, resulting in the increase of the conductivity of the electrode and the corresponding reduction of the interface impedance. Compared with Alg, the cross-linked PAA-PEO binder has a smaller high-frequency impedance and more stable interface impedance. This is because

the cross-linking of PEO with strong conductivity can effectively alleviate the volume expansion of Si anode material, and greatly improve its conductivity. With the number of cycles increasing to 50, the interface impedance corresponding to Si@C@PDA-PAA-PEO is the same as that after 20 cycles. The coincidence of the curves shows that the interface impedance with Si@C@PDA-PAA-PEO is more stable, which is also an important factor because Si@C@PDA-PAA-PEO can keep the long-term stable cycle better than the Si@C@PDA-Alg electrode.

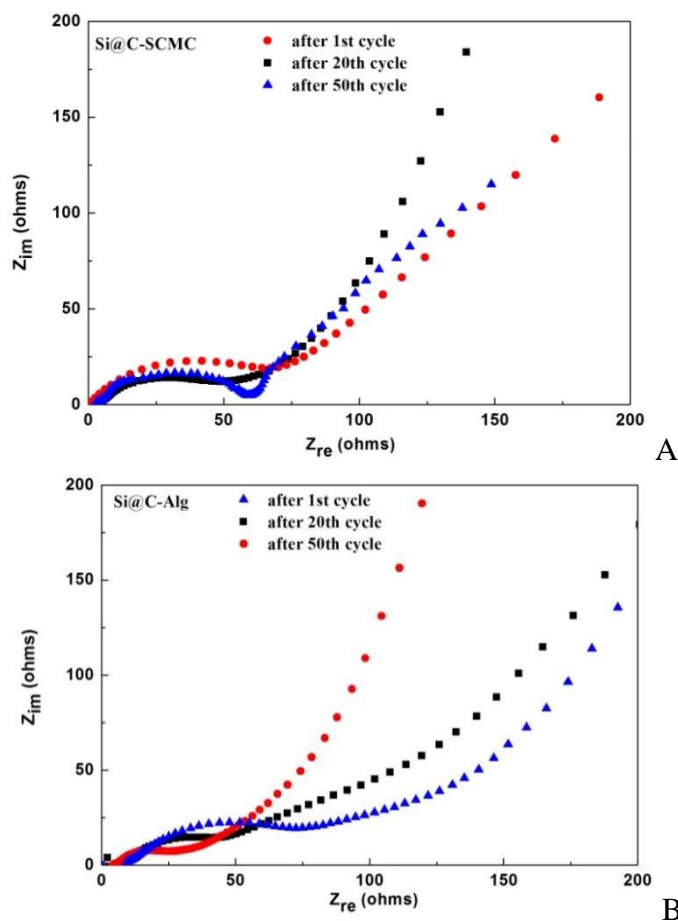


**Figure 8.** AC impedance spectra of Si@C@PDA-Alg and Si@C@PDA-PAA-PEO electrodes after different cycles

### 3.3 Mechanical property characterization

The peel strength of the electrodes prepared with three different binders was tested, as shown in Fig.9.

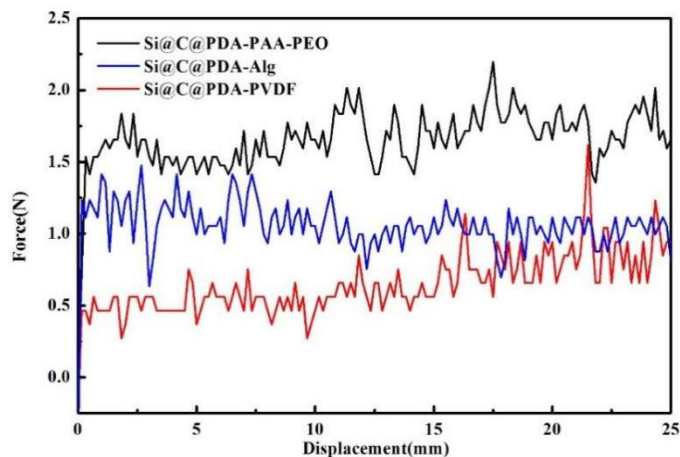


**Figure 9.** Peel strength of the Si@C@PDA-PVDF Si@C@PDA-Alg and Si@C@PDA-PAA-PEO electrodes after different cycles

The peel strength of the electrode can be used to characterize the adhesion of the material. The binder with a strong adhesive force can effectively adhere the active material and conductive agent to the collecting fluid. In the process of charging and discharging, the largest proportion of the active material peeling and the conductive network is destroyed, so as to improve the cycle performance of the battery.

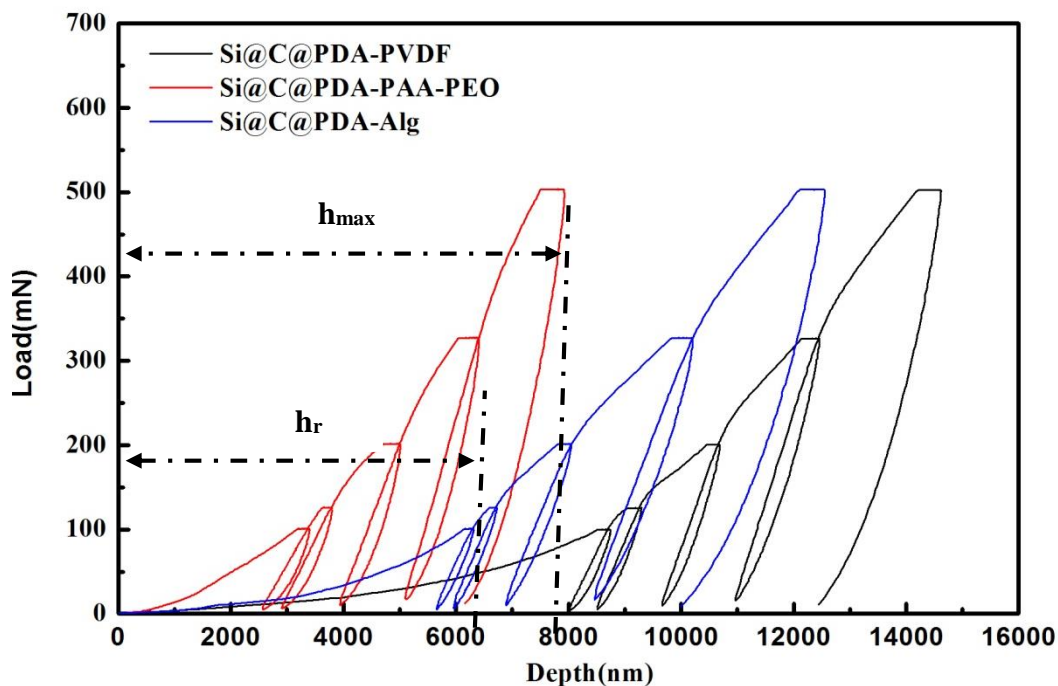


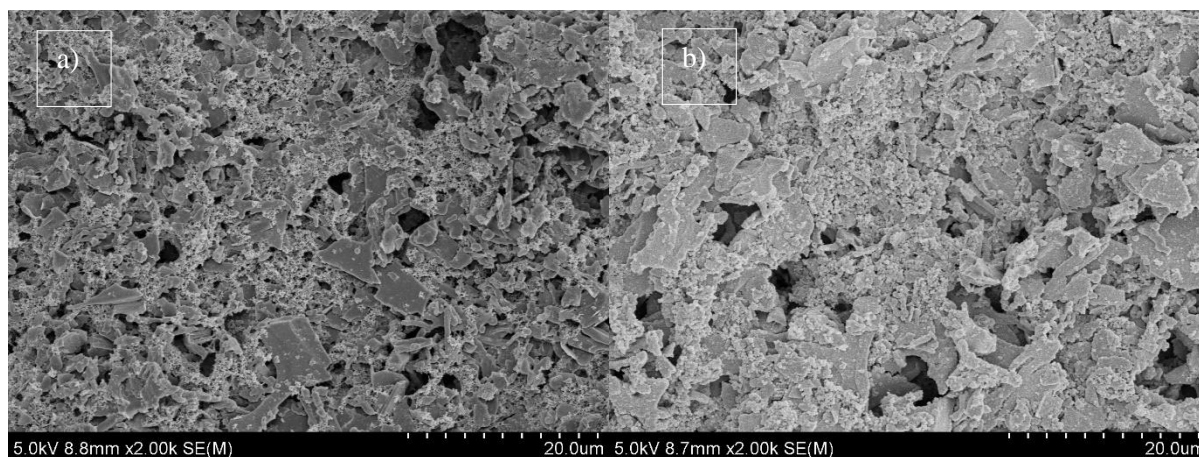
**Figure 10.** Load displacement curve of the pole piece of Si@C@PDA-PVDF, Si@C@PDA-Alg and Si@C@PDA-PAA-PEO

From Fig. 9a), it can be seen that Si@C@PDA-PAA-PEO has the strongest average peel strength,

approximately 2.14 N, which is much higher than the 1.68 N of Alg and 0.98 N of PVDF. From Fig. 9b), it can also be seen clearly that a large number of particles have fallen off from Si@C@PDA-PVDF and Si@C@PDA-Alg, while only a small amount of particles have fallen off at Si@C@PDA-PAA-PEO. Compared with Alg and PVDF, the PAA-PEO cross-linking binder can effectively fix the active material and the conductive agent on the collecting fluid. The catechol functional group in PAA-PEO has a good adhesion, It can be firmly combined with the hydroxyl group in PDA, At the same time, the imine group in PDA can also react with PAA, which transforms the two-dimensional linear bond into a three-dimensional cross-linked bond system, providing excellent mechanical properties for the electrode.

To further compare the mechanical properties of the three kinds of binders, a nanoindentation test was carried out on a negative electrode made of three kinds of binders. As shown in Fig. 10., it can be observed that the indentation depth  $H_{max}$  at the maximum load of the three adhesives and the final depth  $H_r$  at the unloading. The final depth of the Si@C@PDA-PAA-PEO electrode is far less than that of Si@C@PDA-PVDF and Si@C@PDA-Alg, indicating PAA-PEO. It is helpful to resist the stress caused by the expansion and contraction of silicon and avoid damage to the negative structure of silicon. To further prove that the performance of Si@C@PDA-PAA-PEO is better than that of Si@C@PDA-Alg and Si@C@PDA-PVDF, we performed SEM scanning analysis on the electrodes coated with three kinds of binders and the electrodes after 200 cycles, as shown in Fig. 11.

The above viewpoint is further proven by comparison, as shown in Fig. 11a) b). The electrode particles of Si@C@PDA-PAA-PEO before and after circulation were unchanged, the volume expansion was not very obvious, and the distribution was uniform. Figure 11c) d) shows the comparison diagram of Si@C@PDA-Alg before and after the cycle. It can be seen from the figure that after a long cycle, although there is no obvious crack on the Si@C@PDA-Alg electrode, the volume expansion is very serious, and the particles become very thick. Fig. 11e) f) shows the comparison diagram of Si@C@PDA-PVDF before and after the cycle. It can be seen from the figure that after a long cycle, there are obvious cracks in the material, which is caused by the crystallization phenomenon of PVDF during the charging and discharging process as the binder reduces its bonding strength. With the constant change of the volume of Si@C composite negative electrode material, the binder cannot bear the volume expansion of the negative electrode material, resulting in the rupture or even fall off of the material and copper foil. This conclusion further shows that PAA-PEO is more suitable for Si@C composite anode materials.



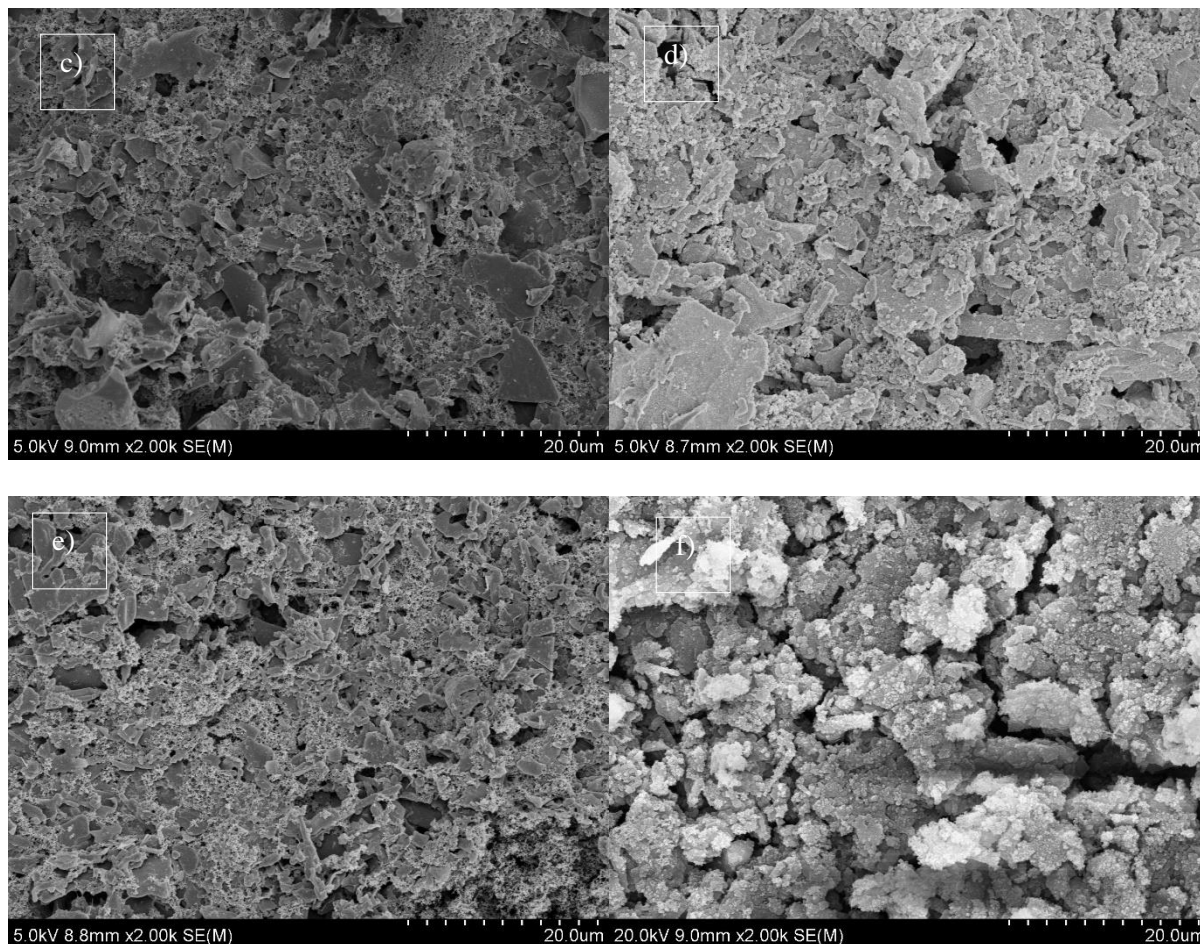


**Figure 11.** SEM photos of Si@C electrodes prepared by different coated carbon sources before and after cycling (a)(b) before and after cycling of Si@C-PDA (c)(d) before and after cycling of Si@C-PVDF (e)(f) before and after cycling of Si@C-C<sub>6</sub>H<sub>12</sub>O<sub>6</sub>

We prepared a PAA-PEO cross-linking binder Si@C@PDA-PAA-PEO negative electrode material. The comparison with the negative electrode material prepared by the binder mentioned in other literature is shown in the table below.

**Table 1.** Comparison of various anode materials for Li-ion batteries.

binder	Capacity(Cycle number) (mAhg <sup>-1</sup> )	Current Density (mAhg <sup>-1</sup> )	bond strength(N)	Reference
PAA-PEO	2500(600)	200	2.14	This Work
Alg	2000(300)	200	0.98	[3]
PAA	2500(300)	200	1.0	[22]
PVDF	2140(30)	50	0.63	[23]

The cycle performance, cycle times, and bond strength were compared. The results show that under a high current density, the Si@C@PDA-PAA-PEO composite anode material prepared by this

method has a higher capacity and cycle stability at a high current density than other materials reported in other literature. This shows that PAA-PEO as a binder has good application prospects for silicon cathode materials.

#### 4. CONCLUSIONS

In this paper, PAA-PEO was prepared by copolymerization, and a layer of PDA was self-polymerized on the surface of Si@C by hydrogen bonding. Si@C@PDA-PAA-PEO negative electrode materials were successfully prepared and compared with the negative electrode material prepared by the traditional binder Alg and PVDF. The results show that the cross-linked binder PAA-PEO can be well combined with PDA to form a stable structure. Compared with the traditional binder, PAA-PEO has stronger adhesion and deformation resistance. Under a current density of  $1000 \text{ mA g}^{-1}$ , the capacity of  $600 \text{ mA g}^{-1}$  can be kept stable for 200 cycles. The addition of PEO significantly improves the ionic conductivity of the battery and provides a promising environmental binder for the next generation of lithium-ion batteries.

#### ACKNOWLEDGEMENTS

This work was supported by the Doctoral research start-up fund (JMSUBZ2020-01).

#### References

1. L.S. Hao, Z.P. Cai, L. Wei-Shan, *J. Power Sources*, 34(2010)303.
2. X. Shen, Z. Tian, R. Fan, L. Shao, D. Zhang, G. Cao, L. Kou and Y. Bai, *J. Energy Chem.*, 27(2018) 24.
3. J. Bae, S.H. Cha, J. Park, *Macromol. Res.*, 21(2013)826.
4. S.L. Chou, Y. Pan, J.Z. Wang, H.K. Liu and S.X. Dou, *Phys. Chem. Chem. Phys.*, 16(2014)20347.
5. M. Ling, J. Qiu, S. Li, H. Zhao, G. Liu and S. Zhang, *J. Mater. Chem. A*, 1(2013)11543.
6. H. Buqa, M. Holzapfel, F. Krumeich, C. Veit and P. Novák, *J. Power Sources*, 161(2006)617.
7. H.K. Park, B.S. Kong, E.S. Oh, *Electrochem. Commun.*, 13(2011)1051.
8. K. Igor, Z. Bogdan, M. Alexandre, H. Benjamin, M. Zoran, B. Ruslan, L. Igor and Y. Gleb, *Science*, 334(2011)75.
9. S. Choi, T.W. Kwon, A. Coskun, J.W. Choi, *Science*, 357(2017)279.
10. L. Shen, Z. Wang, L. Chen, *ChemSusChem*, 7(2014)1951.
11. C. Chen, H.L. Sang, M. Cho, J. Kim and Y. Lee, *ACS Appl. Mater. Interfaces*, 8(2016)2658.
12. J. Song, M. Zhou, R. Yi, T. Xu, M.L. Gordin, D. Tang, Z. Yu, M. Regula and D. Wang, *Adv. Funct. Mater.*, 24(2014)5904.
13. S. Lim, H. Chu, K. Lee, T. Yim, Y. Kim, J. Mun and T. Kim, *ACS Appl. Mater. Interfaces.*, 7(2015) 23545.
14. J. Zhao, Y. Su, X. He, X. Zhao, Y. Li, R. Zhang and Z. Jiang, *J. Membr. Sci.*, 465(2014)41.
15. K. Amine, R. Kanno, Y.T. Zeng, *MRS Bull.*, 39 (2014) 395.
16. Y. Shi, R. Jiang, M. Liu, L. Fu, G. Zeng, Q. Wan, L. Mao, F. Deng, X. Zhang and Y. Wei, *Mater. Sci. Eng., C*, 77(2017)972.
17. J.L. Shi, L.F. Fang, H. Li, H. Zhang, B.K. Zhu and L.P. Zhu, *J. Membr. Sci.*, 437(2013)160.
18. Y. Luo, Q. Ran, S. Wu, J. Shen, *J. Appl. Polym. Sci.*, 109(2008)3286.

19. L. Lü, H. Lou, Y. Xiao, G. Zhang, C. Wang and Y. Deng, *RSC Adv.*, 8(2018)4604.
20. M. Ling, J. Qiu, S. Li, C. Yan, M.J. Kiefel, G. Liu and S. Zhang, *Nano Lett.*, 15(2015)4440.
21. Y. Park, S. Lee, S.H. Kim, B.Y. Jang, J.S. Kim, S.M. Oh, J.Y. Kim, N.S. Choi, K.T. Lee and B.S. Kim, *RSC Adv.*, 3(2013)12625.
22. S.H. Ng, J. Wang, D. Wexler, S.Y. Chew and K.L. Hua, *J.Phys.Chem.C*, 111(2007)11131.
23. M. Ling, Y. Xu, H. Zhao, X. Gu, J. Qiu, S. Li, M. Wu, X. Song, C. Yan and G. Liu, *Nano Energy*, 12(2015)178.

© 2022 The Authors. Published by ESG ([www.electrochemsci.org](http://www.electrochemsci.org)). This article is an open access article distributed under the terms and conditions of the Creative Commons Attribution license (<http://creativecommons.org/licenses/by/4.0/>).